The North Atlantic Eddy Heat Transport and Its Relation with the Vertical Tilting of the Gulf Stream Axis

A. M. TREGUIER AND C. LIQUE

Laboratoire d'Océanographie Physique et Spatiale, CNRS-IFREMER-IRD-UBO, IUEM, Plouzane, France

J. DESHAYES

Sorbonne Universités (UPMC)-CNRS-IRD-MNHN, LOCEAN Laboratory, Paris, France

J. M. MOLINES

CNRS-University Grenoble Alpes, Laboratoire de Glaciologie et Géophysique de L'environnement, Grenoble, France

(Manuscript received 26 July 2016, in final form 12 March 2017)

ABSTRACT

Correlations between temperature and velocity fluctuations are a significant contribution to the North Atlantic meridional heat transport, especially at the northern boundary of the subtropical gyre. In satellite observations and in a numerical model at $^1/_{12}°$ resolution, a localized pattern of positive eddy heat flux is found northwest of the Gulf Stream, downstream of its separation at Cape Hatteras. It is confined to the upper 500 m. A simple kinematic model of a meandering jet can explain the surface eddy flux, taking into account a spatial shift between the maximum velocity of the jet and the maximum cross-jet temperature gradient. In the Gulf Stream such a spatial shift results from the nonlinear temperature profile and the vertical tilting of the velocity profile with depth. The numerical model suggests that the meandering of the Gulf Stream could account, at least in part, for the large eddy heat transport (of order 0.3 PW) near 36°N in the North Atlantic and for its compensation by the mean flow.

1. Introduction

At midlatitudes, the atmospheric heat transport is performed by transient disturbances, large-scale cyclones, and anticyclones, as discussed, for example, by Kuo (1956). At the same latitudes, in the ocean, both the time-mean circulation and the transient eddies contribute to the meridional heat transport (Smith et al. 2000). The importance of the time-mean circulation, in the case of the oceanic heat transport, is due to the existence of large-scale currents such as the Gulf Stream, which flows poleward along the western boundary of the North Atlantic. The oceanic heat transport can be inferred from air–sea surface fluxes (Large and Yeager 2009), and these estimates show that despite its relatively small width compared to the Pacific, the Atlantic Ocean performs half the global oceanic heat transport in the 20°–40°N latitude range. This has been recently confirmed at 26.5°N by the in situ measurements of the RAPID array, which gave an Atlantic heat transport of 1.25 ± 0.36 PW over 8 years (McCarthy et al. 2015).

This paper is focused on the eddy heat transport, namely, the time average of the product of velocity and temperature temporal fluctuations. In our definition, "eddy" includes all the time variability at periods larger than a few days; this variability consists of coherent eddies but also waves, meanders, and large-scale modes of variability. With this definition, the eddy heat transport is small at the latitude of RAPID: 0.08 ± 0.03 PW (McCarthy et al. 2015). On the contrary, farther north, downstream of the Gulf Stream separation, satellite observations of surface temperature and geostrophic velocity have revealed a large, localized eddy heat flux (Zhai and Greatbatch 2006). These authors have estimated an equivalent horizontal eddy diffusivity of 1000 to 2000 $m^2 s^{-1}$ for this eddy flux, but they have not investigated its origin further.

Corresponding author: A. M. Treguier, treguier@ifremer.fr

DOI: 10.1175/JPO-D-16-0172.1

Estimating the eddy contribution to heat transport over the whole North Atlantic requires knowledge of the time-evolving, three-dimensional velocity and temperature fields, information that only high-resolution numerical simulations can provide. Since the pioneering study of Smith et al. (2000), numerical models at resolutions of 1/10° or higher have been used to estimate the meridional heat transport in the Atlantic Ocean. These models all suggest that the eddy heat transport is largest in the 35°–40°N latitude band. There it can exceed 0.3 PW and accounts for one-quarter to one-third of the total meridional heat transport (Smith et al. 2000; Hecht and Smith 2008; Treguier et al. 2012). This contrasts with lower-resolution models, such as the Parallel Ocean Climate Model (POCM) model with 1/2° resolution at the equator analyzed by Jayne and Marotzke (2002), where the eddy heat transport is lower (0.1 PW, one-tenth of the total, at 40°N). Comparing numerical models at increasing resolution, Hecht and Smith (2008) and Treguier et al. (2012) find that the total meridional heat transport increases with resolution, but they also note that at most latitudes the increase is due to changes in the time-mean circulation more than an increase of the eddy transport. Indeed, an increased contribution of transient eddies at a given latitude does not necessarily cause a larger total transport: the time-mean flow is modified at higher resolution, in such a way that eddy and time-mean flow contributions tend to compensate each other, as demonstrated by Cox (1985) and further discussed by Bryan (1986).

The dynamics of the Gulf Stream and its eddy fluxes are often considered in the framework of a free eastward jet subject to baroclinic instability. In the classical models, such as Phillips or Charney's (e.g., Pedlosky 1979), instability leads to the development of waves and eddies and thus generates a cross-jet eddy heat flux that tends to reduce the temperature gradient across the front. However, the Gulf Stream is a western boundary current, much more complex than a free zonal jet. In a recent analysis based on a high-resolution model (7-km grid), Kang and Curchitser (2015) have considered separately three regions with different dynamics, upstream and downstream of the Gulf Stream separation from the coast, and confirmed that both barotropic and baroclinic energy conversions are active. However, they have not analyzed the heat balance or eddy heat fluxes.

Here, we use recent satellite observations and 1/12° model simulations to understand the origin of the eddy heat flux in the 35°–40°N latitude band. We argue that the structure of the Gulf Stream, and more precisely the spatial shift between velocity and temperature, plays a key role in the generation of a localized eddy flux, which has a significant contribution to the total meridional heat transport in the Atlantic.

2. Methods

We use a classical eddy mean decomposition, defining the "mean" as a time average. Being the product of velocity v and temperature T, the time-averaged heat transport results from the sum of two terms:

$$\overline{vT} = \overline{v}\,\overline{T} + \overline{v'T'}, \tag{1}$$

where time averages are represented by overbars, and deviations from the average are denoted by primes.

Following Zhai and Greatbatch (2006), we compute the eddy flux $\overline{v'T'}$ at the ocean surface, using satellite data. The sea surface temperature is obtained from NOAA (Reynolds et al. 2007), and the geostrophic velocity is produced by SSALTO/DUACS and distributed by AVISO, with support from CNES (http://www.aviso.altimetry.fr/duacs/). Both products have a daily frequency and are distributed on the same 1/4° grid. We also use a numerical simulation performed in the framework of the Drakkar project (Barnier et al. 2014) with the ORCA12 model. It is based on the NEMO modeling framework (Madec 2008) for the ocean and sea ice. The isotropic tripolar grid covers the global ocean with a resolution of 1/12° (9.3 km) at the equator, refined at higher latitudes (6.5 km at 45°, 1.8 km in the Ross and Weddell seas). The atmospheric forcing, the Drakkar forcing set (DFS4.4), is an updated version of the Drakkar forcing sets described by Brodeau et al. (2010). The ORCA12 simulation is forced by an interannually varying atmosphere over the period 1958–2012. The 5-day averages of model variables are stored and used to diagnose eddy fluxes. The atmospheric temperature, humidity, and winds are prescribed as well as the downward radiative fluxes. Turbulent heat fluxes and outgoing longwave radiation are calculated using the model sea surface temperature and bulk formulas. This is equivalent to a restoring surface flux coefficient of about 40 $\mathrm{W\,m^{-2}\,K^{-1}}$ in the North Atlantic (Barnier et al. 1995). Further details as well as validations with observations are found in Serazin et al. (2015), who used ORCA12 to estimate the intrinsic variability of the sea level, and in Barrier et al. (2015), who studied the interannual variability of the North Atlantic Subpolar Gyre. The Gulf Stream dynamics in our 1/12° models have been studied in detail by Maze et al. (2013), who analyzed the potential vorticity budget of the 18°C water in an earlier regional version of the Drakkar model. The analysis of eddy fluxes of salt in the same regional configuration by Treguier et al. (2012) has motivated the present investigation of the eddy heat flux.

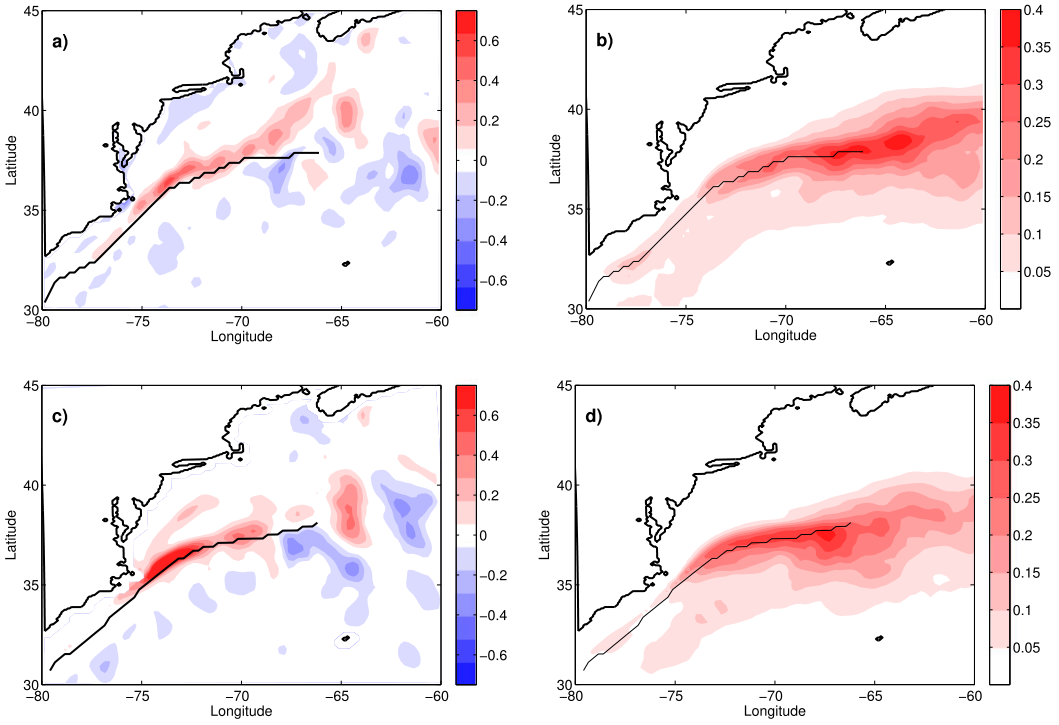

FIG. 1. (left) Map of surface eddy flux $\overline{v'T'}$ (°C m s^{-1}) computed from (a) observations and the (c) ORCA12 model. The black line represents the Gulf Stream axis (maximum time-mean velocity module). (right) Eddy kinetic energy (m^2 s^{-2}) from (b) Aviso observations and the (d) ORCA12 model. All quantities are averaged over the period 2003–12.

3. Structure of the eddy heat transport near the Gulf Stream separation

The surface meridional eddy flux $\overline{v'T'}$ is computed from observations (Fig. 1a) and model (Fig. 1c), averaged over the same 10-yr period (2003–12). The observations, which cover a longer and more recent period than Zhai and Greatbatch (2006), confirm their findings. In Fig. 1a, an elongated patch of positive $\overline{v'T'}$ is found, downstream of the Gulf Stream separation at Cape Hatteras. It is located north of the Gulf Stream axis, which is defined as the maximum surface velocity module in the AVISO data (black line in Fig. 1a). The location of the eddy flux does not coincide with the maximum eddy kinetic energy that occurs farther downstream (Fig. 1b) in the region of the most active meanders and eddies. We present in Fig. 1 only the meridional component of the eddy flux, which contributes directly to the meridional heat transport integrated over the Atlantic basin. Zhai and Greatbatch (2006) considered the vector flux and showed that it is oriented to the northeast. They verified that this pattern was not due to the rotational part of the flux (which would have no impact on the eddy–mean flow interactions) and quantified the contribution from the surface Ekman velocities (which they found negligible). This pattern of positive $\overline{v'T'}$ northwest of the Gulf Stream axis is reproduced by the ORCA12 model (Fig. 1c), with a somewhat larger amplitude. In the model, as in the observations, the stronger positive $\overline{v'T'}$ values are found upstream of the region of highest eddy kinetic energy (Fig. 1d).

The numerical model reveals the vertical structure of the eddy heat flux (Fig. 2, top) and demonstrates that it is not restricted to the surface mixed layer. The section of $\overline{v'T'}$ at 36°N, near the Gulf Stream separation from the coast, shows at all depths above 500 m a large positive eddy flux located to the west of the maximum velocity. Note that the line of maximum velocity is tilted and moves offshore as a function of depth. This asymmetry of the velocity profile appears clearly in Fig. 2 (bottom), where the time-mean velocity and isotherms are represented along the same section. The tilted velocity structure of the Gulf Stream is well documented on the continental slope and is reflected in the development of instabilities. Submesoscale instabilities tend to form on the cyclonic side (closest to the coast) as demonstrated recently by Gula et al. (2015). The tilted structure of the model velocity profile, with a larger velocity gradient on the cyclonic side,

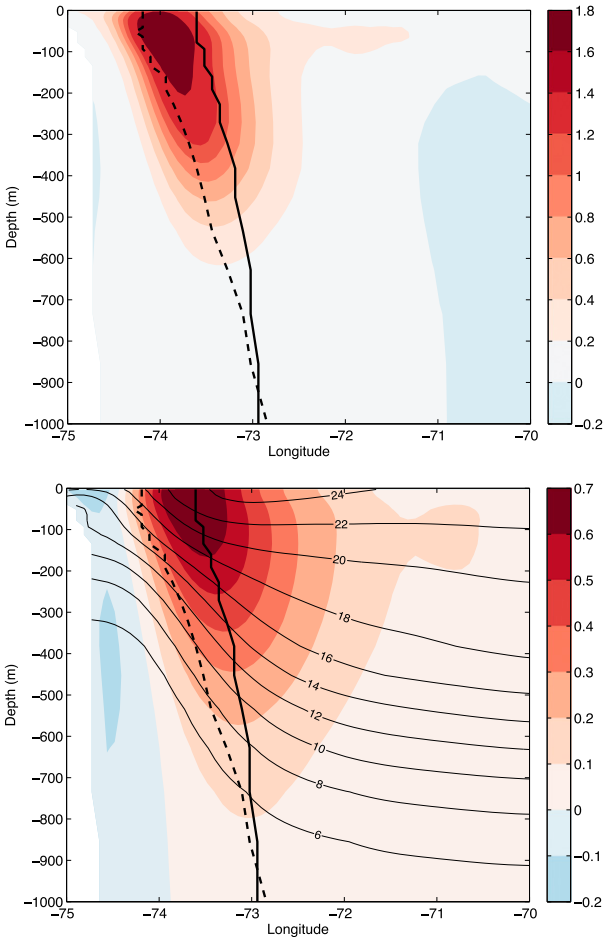

FIG. 2. (top) Section of eddy $\overline{v'T'}$ (°C m s^{-1}) at 36°N in ORCA12. (bottom) Time-mean meridional velocity (color; m s^{-1}) and temperature (contours; °C). In both panels, the thick black line shows the location of the maximum meridional velocity, and the dashed line represents the location of the maximum zonal temperature gradient. All quantities are averaged over the period 2003–12.

agrees with the velocity profiles observed just downstream of Cape Hatteras by Rossby (1987) and more recently by Toole et al. (2011). The vertical tilting has been analyzed by Ratsimandresey and Pelegri (2005), who show that it appears when the velocity is plotted as a function of depth, while the tilting disappears when velocity is plotted as a function of density (or temperature). As a consequence of this tilting the maximum temperature gradient in the upper layers [dashed line in Fig. 2 (bottom)] does not coincide with the velocity maximum; it is located to the west (closer to the coast). To see this, let us consider the thermal wind relation in two-dimensional Cartesian coordinates, with a meridional velocity v, temperature T, Coriolis parameter f, gravitational acceleration g, and thermal expansion coefficient α:

$$\frac{\partial}{\partial z}v(x,z)=\frac{\alpha g}{f}\frac{\partial}{\partial x}T(x,z). \tag{2}$$

Integrating in z and taking the derivative in x, one obtains

$$\frac{\partial}{\partial x}v(x,z)=\frac{\partial}{\partial x}v(x,-H)+\frac{\alpha g}{f}\int_{-H}^{z}\frac{\partial^2}{\partial x^2}T(x,z)\,dz. \tag{3}$$

At a given depth z, the lhs of (3) vanishes at the longitude of maximum velocity $x_m(z)$. If the location of the maximum temperature gradient changes with depth (is tilted), there is no reason for this longitude $x_m(z)$ to correspond to the longitude of the maximum temperature gradient at the same depth, due to the vertical integral on the right-hand side.

Such a spatial shift between the maximum velocity and the maximum temperature gradient is probably present in the observations of Rossby (1987), but it is marginally resolved by the spacing between the profiles (24 km); it seems present in Fig. 2 of Toole et al. (2011). The characteristic shape of the vertical profiles in Fig. 2 was found in the earlier simulations analyzed by Treguier et al. (2012) and Treguier et al. (2014). It is likely that all models with high enough resolution reproduce this observed feature of the Gulf Stream, although this has not been documented in the literature.

4. Mechanisms of eddy heat transport

What source of variability can be responsible for the localized $\overline{v'T'}$ pattern just downstream of Cape Hatteras? Although barotropic and baroclinic instability are the physical mechanisms that cause the Gulf Stream to vary in time and produce eddy fluxes, these theories do not provide a simple explanation for the localized patch of $\overline{v'T'}$ correlations pictured in Figs. 1 and 2. The Gulf Stream starts meandering after its separation at Cape Hatteras (e.g., Watts and Johns 1982), but the largest meanders and ring shedding occur farther downstream. In observations, as in the realistic simulation (Fig. 1), the eddy fluxes are at their maximum where the Gulf Stream starts to meander, right after its separation from the coast. The generation of eddy heat fluxes by an analytical meandering jet has been examined by Jayne and Marotzke (2002). They found that meandering resulted in symmetric positive and negative patterns, which cancelled out when integrated over a meander wavelength. They concluded that "there is no divergent part of the eddy heat transport due to a coherent meandering jet, regardless of its relative functional form and irrespective of its meander mode. All of the eddy heat transport due to a meandering structure is therefore

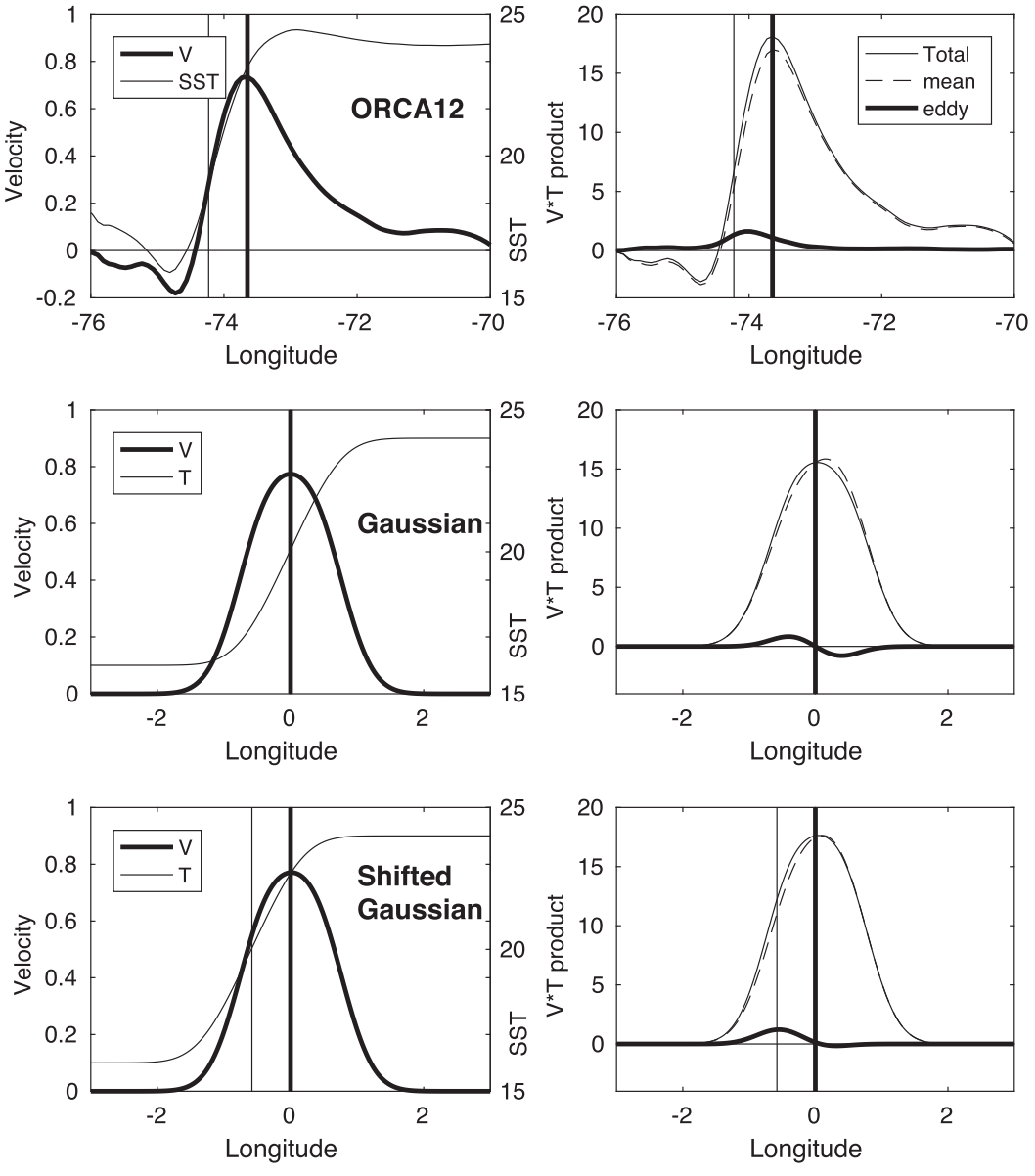

FIG. 3. (top) Surface meridional velocity and SST at 36°N in ORCA12 as a function of longitude. (left) Time-mean surface velocity (left axis; $m\,s^{-1}$) and SST (right axis; °C). (right) Total, time mean, and eddy velocity–temperature products ($°C\,m\,s^{-1}$). In all panels, the vertical lines mark the longitude of maximum velocity (thick line) and the longitude of maximum temperature gradient (thin line). The middle and bottom rows show the same quantities for an analytical Gaussian meandering jet, with the time-mean defined on a meander period, in the same units (see text). (middle) The case of a tracer gradient centered on the jet axis; positive and negative eddy fluxes on each side of the velocity maximum cancel out when integrated over the x axis. (bottom) The maximum velocity is shifted to the right of the maximum tracer gradient and there is a net positive eddy flux integrated across the jet, as simulated by ORCA12.

rotational" (Jayne and Marotzke 2002, p. 3335). They did not, however, consider the case of a jet with a shift between the velocity and the temperature profiles.

The top two panels of Fig. 3 show the surface temperature, meridional velocity, and their correlation at 36°N in the ORCA12 simulation. The shift in longitude between the maximum temperature gradient and the maximum velocity is 0.58°. Regarding the origin of this shift at the surface, (3) shows that in a geostrophic current it may be due to the reference velocity $v(x, -H)$ or to the tilting with the depth of the maximum temperature gradient, that is, its origin can be barotropic or

baroclinic. For ORCA12, in the region shown in Fig. 3, the barotropic velocity is 10% of the surface velocity, and the shift is mainly baroclinic. In the top-right panel of Fig. 3, the eddy temperature–velocity correlation is positive. Locally, the eddy term appears small compared to the mean, but the mean includes a nondivergent component that would cancel out in a basinwide average. For this reason, the eddy to mean ratio is not significant in this small region, although the eddy flux itself is relevant, as will be shown in section 5. Assuming that the eddy temperature–velocity correlation keeps the same amplitude over the top 300 m of the water column, we can compute an equivalent heat flux. The integral over the longitude band 76°–70°W is 0.25 PW, comparable to the basinwide eddy heat flux in ORCA12 as well as in other numerical models (Smith et al. 2000; Hecht and Smith 2008; Treguier et al. 2012).

A simple kinematic model demonstrates that a spatial shift between temperature and velocity can produce such a net positive eddy heat flux in a meandering jet. We consider a Gaussian jet with velocity v:

$$v = v_0 \exp(-x_v^2/L^2). \tag{4}$$

The direction x is perpendicular to the jet axis, v_0 is the velocity amplitude, and L is the jet width. We assume that the jet axis meanders sinusoidally with typical amplitude x_m, as a function of time t, so that the argument x_v is a function of x and t:

$$x_v(x,t) = x - x_m \cos(\omega t). \tag{5}$$

Let us assume further that a tracer gradient exists across the jet, with the same Gaussian structure as the jet (a logical hypothesis if the jet is geostrophic). The tracer distribution is the integral of this gradient:

$$T = T_0 + \delta T \mathrm{erf}(x_v/L). \tag{6}$$

We choose parameters close to the ORCA12 solution at the surface because this is where the shift is largest: $T_0 = 16°C$, $\delta T = 8°C$, $v_0 = 1.2\,\mathrm{m\,s^{-1}}$, and jet width $L = 0.58°$. We assume that the meander width x_m is equal to L. The velocity and tracer averaged over one meander period are plotted in Fig. 3 (middle-left row). Note that if the meander width was much larger than the jet width, the time-mean velocity would exhibit two peaks rather than a single one. Our choice of parameters is meant to produce a qualitative agreement with the ORCA12 model, where the mean velocity has a single maximum. The tracer transport $\overline{vT}$ and its mean and eddy decomposition $\overline{v}\,\overline{T}$ and $\overline{v'T'}$ are shown in the middle-right row of Fig. 3. In this example, the tracer gradient across the jet is perfectly centered on the jet axis, contrary to the ORCA12 model. The eddy flux of the tracer is antisymmetric about the jet axis, with positive values on one side and negative values on the other side, resulting in a negligible net eddy contribution integrated across the jet in agreement with Jayne and Marotzke (2002). On the left of the mean jet axis, meanders bring positive temperature anomalies, resulting in a positive $\overline{v'T'}$, while they bring negative temperature anomalies on the right side. Note that the cancellation between positive and negative fluxes occurs irrespective of the orientation of the jet relative to the section; the jet crossing the section at an angle would produce the same result.

Now let us consider the case when the maximum tracer gradient is shifted to the left of the maximum velocity by a distance δx. Let us define x_t:

$$x_t(x,t) = x - x_m \cos(\omega t) + \delta x. \tag{7}$$

The tracer distribution is now given by (6) with x_t as argument instead of x_v. We take $\delta x = 0.58°$ to fit the ORCA12 model. The resulting time-mean velocity, temperature, and their correlations are shown in Fig. 3 (bottom row). With the shift between the velocity and temperature gradient, the eddy flux is no longer symmetric, and there is a net positive eddy flux across the jet. Its order of magnitude is similar to the one diagnosed in ORCA12; the eddy correlation, integrated over longitude and over a depth of 300 m, would generate a total eddy heat transport of 0.26 PW. Thus, in this case of noncoincident maximum velocity and temperature gradient, when the jet meanders, the eddy/mean decomposition based on the time average gives a significant eddy flux integrated across the jet. This eddy contribution is compensated by a change in the mean tracer flux so that the total remains the same as in the absence of meanders. We think that this simple kinematic model is relevant to explain eddy fluxes of heat and salt in the model Gulf Stream near its separation from the coast. It demonstrates that a meandering jet can produce transient eddy fluxes, provided that a spatial shift exists between the velocity and tracer gradient structures [a case not investigated by Jayne and Marotzke (2002)]. This may also explain why the eddy fluxes are at their maximum near the Gulf Stream separation because although both meander amplitude and eddy kinetic energy increase downstream, the jet becomes less asymmetric where it flows in open water far from the continental slope, and the shift between the maximum velocity and temperature gradient is reduced.

Of course, the Gulf Stream in the ORCA12 model has a more complex behavior than just a regular meandering. Hovmöller diagrams of surface temperature and velocity (not shown) display irregular meanders and variability at

multiple time scales. The sea surface temperature also exhibits a strong seasonal cycle (although this seasonal cycle has a small impact, less than 10%, on the peak of maximum $\overline{v'T'}$ correlation). Furthermore, the velocity in ORCA12 has a more complex shape than a Gaussian, as appears clearly in Fig. 3. For these reasons, although the kinematic model captures the amplitude of eddy temperature correlations at the surface (Fig. 3), a quantitative agreement is more difficult to achieve when a two-dimensional section (x, z) is considered. The temperature field can be defined as a function of depth, and the velocity can be calculated as the sum of a geostrophic velocity and a barotropic reference velocity. In that case we find that a regularly meandering Gaussian jet can account for 25% of the total ORCA12 heat transport, but we have not explored the parameter space further. Here, the kinematic model is used merely to illustrate a contribution to eddy heat transport. One should not expect it to reproduce the complex dynamics of the Gulf Stream separation.

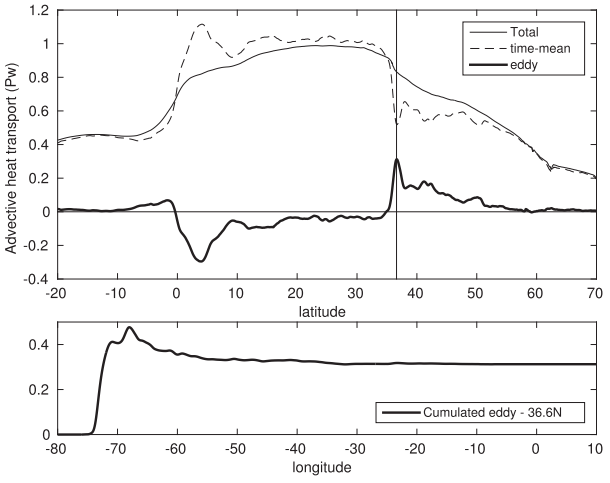

FIG. 4. Meridional heat transport in the Atlantic Ocean averaged over 10 years (2003–12) in the ORCA12 global high-resolution ocean simulation (PW). (top) Total advective transport, with its decomposition into a transport by the time-mean flow and by the transient eddy motions. The vertical line marks the latitude 36.6°N. (bottom) Eddy heat transport at 36.6°N as a function of longitude, cumulated from the west.

5. Consequences for the Atlantic meridional heat transport

Although localized near the western boundary, the eddy heat flux pattern pictured in Fig. 1 is a significant contribution to the meridional heat transport integrated over the basin in the numerical model. The total meridional heat transport in the North Atlantic, averaged over the years 2003–12, is presented as a function of latitude in Fig. 4 with its decomposition into mean and eddy (top). The total heat transport, reaching a maximum of 1 PW, is quite realistic, in the lower range of uncertainty of the RAPID observations at 26°N (Johns et al. 2011; McCarthy et al. 2015).

As appears from the thick line in Fig. 4, the main effect of the eddy $\overline{v'T'}$ in the North Atlantic is to flux heat out of the subtropical gyre, with a southward transport reaching 0.3 PW near 5°N and a northward transport of a similar amplitude in the 35°–40°N latitude band. This structure of the eddy heat transport as a function of latitude is extremely robust. It appears in all eddying models, with maximum values that tend to grow with increasing model resolution (Smith et al. 2000; Hecht and Smith 2008; Volkov et al. 2008; Treguier et al. 2012). The same structure, with an amplitude of about 0.2 PW, was estimated by Stammer (1998) using temperature gradient observations, combined with an eddy diffusion coefficient computed from altimetry data. Note that the importance of the eddy flux across a section depends on the orientation of the mean flow relative to the section. The intergyre eddy heat flux across the Gulf Stream and the North Atlantic Current has been quantified by Hall et al. (2004), following the North Atlantic current path, at the boundary between the subtropical and the subpolar gyre, using a 1/6° model. Across the mean intergyre boundary the eddy heat flux was 0.7 PW, and this was probably underestimated considering the relatively low resolution of the numerical model. Such a large intergyre eddy flux does not appear in the meridional heat transport integrated along latitude lines (Fig. 4) because the latitude lines are not parallel to the mean flow.

Here, we focus on the latitude band corresponding to the Gulf Stream separation. There is a sharp increase (divergence) of the eddy heat flux in that latitude range, with the eddy flux increasing from a small negative value at 33°N to reach a maximum of 0.31 PW at 36.6°N. Our new simulation confirms the finding of Treguier et al. (2012); this large eddy heat flux is due to the dynamics at the western boundary. This appears very clearly when the eddy heat transport at that latitude is plotted, cumulated from the west, as a function of longitude (Fig. 4, bottom). The eddy heat transport quickly reaches a large value within 5° from the coast, due to the positive pattern of $\overline{v'T'}$ pictured in Figs. 1 and 2. Contributions farther east only contribute to a decrease, which brings the cross-basin eddy transport to 0.31 PW.

6. Conclusions

We have confirmed, in observations and a numerical model, the result of Zhai and Greatbatch (2006); there

is a large positive eddy heat flux northwest of the Gulf Stream axis, right after its separation from the coast at Cape Hatteras. This localized positive $\overline{v'T'}$ pattern is not associated with an equally strong negative pattern on the other side of the Gulf Stream axis, thus generating a net basinwide eddy heat flux exceeding 0.3 PW at these latitudes. The meandering of the Gulf Stream as its separates from the coast seems the most likely explanation for this eddy heat flux, taking into account a phase shift between temperature and velocity related to the vertical tilting of the Gulf Stream axis. Note that phase shifts between the maximum temperature variance and the velocity structure have been recently documented in eddies worldwide by Hausmann and Czaja (2012), who have quantified their impact on the eddy heat transport (a contribution which they call "swirl" heat transport). They find it especially large in the Antarctic Circumpolar Current, up to 0.2 PW. To our knowledge, the effect of such phase shifts had not been considered before in the case of a meandering jet. In the Gulf Stream, the mechanism described here for heat transport also explains the large eddy salt flux described at the same location by Treguier et al. (2012).

Our simple kinematic model implies a large compensation between time-mean and transient eddy flux. The analytical meandering jet has the same transport of tracer, whether it meanders or not, but the phase shift between the jet axis and the temperature profile causes a nonzero anomaly in the transport by the time-mean flow that compensates the transient eddy transport. The kinematic model is overly simplified, ignoring dynamics and diabatic mixing, but it is interesting to note that the same behavior occurs in ORCA12. A similar compensation between eddy and mean heat transport appears clearly in the basin-averaged meridional heat flux (Fig. 4). A large eddy mean cancellation in that latitude band is found not only in ORCA12, but also in many other numerical simulations. Consider, for example, the rapid growth of the eddy heat transport from −0.2 to 0.2 PW between 34° and 36°N in the POP 0.1° model (Hecht and Smith 2008): it is not reflected in the total heat transport and must therefore be compensated by a corresponding decrease of the transport by the time-mean flow. This compensation is consistent with our simple kinematic model of the meandering jet. Furthermore, it suggests that this compensation between eddy and mean operates on short time scales (the time scale of a meander). Therefore, if our hypothesis is right, local changes in the characteristics of the Gulf Stream separation in a changing climate would not affect the total heat transport much but would simply modify the repartition between the compensating transient eddy and time-mean transports. More complex mechanisms are certainly at play farther northeast, along the North Atlantic drift at the boundary between the subtropical and the subpolar gyre. There meridional eddy fluxes are likely governed by baroclinic instability, and the relationship between large-scale gradients and eddy fluxes must therefore involve longer time scales (interannual to decadal) with nontrivial consequences for the ocean response to climate change. Finally, the fact that eddy and mean heat fluxes compensate each other locally does not mean that a low-resolution model can represent the Gulf Stream accurately. In noneddying models, the Gulf Stream is laminar and its transport is governed by linear Sverdrup dynamics [with an amplitude of about 30 Sv ($1\ \text{Sv} \equiv 10^6\ \text{m}^3\ \text{s}^{-1}$)]. In high-resolution models, as in the real world, the Gulf Stream transport is enhanced by inertial and eddy rectification mechanisms and exceeds 100 Sv. The nonlinearity of the Gulf Stream has a far-reaching influence on the shape of the subtropical gyre; on the air–sea exchanges of heat, freshwater, and carbon; and on the ocean ecosystems.

Acknowledgments. We thank the reviewers and Paola Cessi, the editor, for their remarks, which helped improve the manuscript. This work is a contribution of the Drakkar project, which is funded by the Centre National de la Recherche Scientifique (CNRS), the Institut National des Sciences de l'Univers (LEFE-INSU), the Groupe Mission Mercator Coriolis (GMMC), and Ifremer. A. M. Treguier acknowledges support from LabexMER (Grant ANR-10-LABX-19-01). The numerical simulation ORCA12.L46-MJM88 presented in this study has been performed at the Centre Informatique National de l'Enseignement Superieur (CINES) computing center, operated by GENCI.

REFERENCES

Barnier, B., L. Siefridt, and P. Marchesiello, 1995: Thermal forcing for a global ocean circulation model using a three-year climatology of ECMWF analyses. *J. Mar. Syst.*, **6**, 363–380, doi:10.1016/0924-7963(94)00034-9.

——, and Coauthors, 2014: DRAKKAR: Developing high resolution ocean components for European Earth system models. *CLIVAR Exchanges*, Vol. 65, International CLIVAR Project Office, Southampton, United Kingdom, 18–21.

Barrier, N., J. Deshayes, A. Treguier, and C. Cassou, 2015: Heat budget in the North Atlantic Subpolar Gyre: Impacts of atmospheric weather regimes on the 1995 warming event. *Prog. Oceanogr.*, **130**, 75–90, doi:10.1016/j.pocean.2014.10.001.

Brodeau, L., B. Barnier, A. Treguier, T. Penduff, and S. Gulev, 2010: An ERA40-based atmospheric forcing for global ocean circulation models. *Ocean Modell.*, **31**, 88–104, doi:10.1016/j.ocemod.2009.10.005.

Bryan, K., 1986: Poleward buoyancy transport in the ocean and mesoscale eddies. *J. Phys. Oceanogr.*, **16**, 927–933, doi:10.1175/1520-0485(1986)016<0927:PBTITO>2.0.CO;2.

Cox, M., 1985: An eddy resolving model of the ventilated thermocline. *J. Phys. Oceanogr.*, **15**, 1312–1324, doi:10.1175/1520-0485(1985)015<1312:AERNMO>2.0.CO;2.

Gula, J., M. J. Molemaker, and J. C. McWilliams, 2015: Topographic vorticity generation, submesoscale instability, and vortex street formation in the Gulf Stream. *Geophys. Res. Lett.*, **42**, 4054–4062, doi:10.1002/2015GL063731.

Hall, N., B. Barnier, T. Penduff, and J. Molines, 2004: Interannual variation of Gulf Stream heat transport in a numerical model forced by reanalysis data. *Climate Dyn.*, **23**, 341–351, doi:10.1007/s00382-004-0449-2.

Hausmann, U., and A. Czaja, 2012: The observed signature of mesoscale eddies in sea surface temperature and the associated heat transport. *Deep-Sea Res. I*, **70**, 60–72, doi:10.1016/j.dsr.2012.08.005.

Hecht, M., and R. Smith, 2008: Towards a physical understanding of the North Atlantic: A review of model studies. *Ocean Modeling in an Eddying Regime*, *Geophys. Monogr.*, Vol. 177, Amer. Geophys. Union, 213–240.

Jayne, S., and J. Marotzke, 2002: The oceanic eddy heat transport. *J. Phys. Oceanogr.*, **32**, 3328–3345, doi:10.1175/1520-0485(2002)032<3328:TOEHT>2.0.CO;2.

Johns, W. E., and Coauthors, 2011: Continuous, array-based estimates of Atlantic Ocean heat transport at 26.5°N. *J. Climate*, **24**, 2429–2449, doi:10.1175/2010JCLI3997.1.

Kang, D., and E. N. Curchitser, 2015: Energetics of eddy–mean flow interactions in the Gulf Stream region. *J. Phys. Oceanogr.*, **45**, 1103–1120, doi:10.1175/JPO-D-14-0200.1.

Kuo, H., 1956: Forced and free meridional circulations in the atmosphere. *J. Meteor.*, **13**, 561–568, doi:10.1175/1520-0469(1956)013<0561:FAFMCI>2.0.CO;2.

Large, W. G., and S. G. Yeager, 2009: The global climatology of an interannually varying air–sea flux data set. *Climate Dyn.*, **33**, 341–364, doi:10.1007/s00382-008-0441-3.

Madec, G., 2008: NEMO ocean engine. Institut Pierre-Simon Laplace Note du Pole de Modélisation 27, 300 pp.

Maze, G., J. Deshayes, J. Marshall, A. Treguier, A. Chronis, and L. Vollner, 2013: Surface vertical PV fluxes and subtropical mode water formation in an eddy-resolving numerical simulation. *Deep-Sea Res. II*, **91**, 128–138, doi:10.1016/j.dsr2.2013.02.026.

McCarthy, G., and Coauthors, 2015: Measuring the Atlantic meridional overturning circulation at 26°N. *Prog. Oceanogr.*, **130**, 91–111, doi:10.1016/j.pocean.2014.10.006.

Pedlosky, J., 1979: *Geophysical Fluid Dynamics*. Springer-Verlag, 624 pp.

Ratsimandresey, A., and J. Pelegri, 2005: Vertical alignment of the Gulf Stream. *Tellus*, **57A**, 691–700, doi:10.1111/j.1600-0870.2005.00115.x.

Reynolds, R. W., T. Smith, C. Liu, D. Chelton, K. Casey, and M. Schlax, 2007: Daily high-resolution-blended analyses for sea surface temperature. *J. Climate*, **20**, 5473–5496, doi:10.1175/2007JCLI1824.1.

Rossby, T., 1987: On the energetics of the Gulf Stream at 73W. *J. Mar. Res.*, **45**, 59–82, doi:10.1357/002224087788400918.

Serazin, G., T. Penduff, S. Gregorio, B. Barnier, J. Molines, and L. Terray, 2015: Intrinsic variability of sea level from global 1/12° ocean simulations: Spatiotemporal scales. *J. Climate*, **28**, 4279–4292, doi:10.1175/JCLI-D-14-00554.1.

Smith, R. D., M. E. Maltrud, F. O. Bryan, and M. Hecht, 2000: Simulation of the North Atlantic Ocean at 1/10°. *J. Phys. Oceanogr.*, **30**, 1532–1561, doi:10.1175/1520-0485(2000)030<1532:NSOTNA>2.0.CO;2.

Stammer, D., 1998: On eddy characteristics, eddy transports, and mean flow properties. *J. Phys. Oceanogr.*, **28**, 727–739, doi:10.1175/1520-0485(1998)028<0727:OECETA>2.0.CO;2.

Toole, J. M., R. G. Curry, T. M. Joyce, M. McCartney, and B. Peña-Molino, 2011: Transport of the North Atlantic deep western boundary current about 39°N, 70°W: 2004–2008. *Deep-Sea Res. II*, **58**, 1768–1780, doi:10.1016/j.dsr2.2010.10.058.

Treguier, A. M., J. Deshayes, C. Lique, R. Dussin, and J. M. Molines, 2012: Eddy contributions to the meridional transport of salt in the North Atlantic. *J. Geophys. Res.*, **117**, C05010, doi:10.1029/2012JC007927.

——, and Coauthors, 2014: Meridional transport of salt in the global ocean from an eddy-resolving model. *Ocean Sci.*, **10**, 243–255, doi:10.5194/os-10-243-2014.

Volkov, D., T. Lee, and L. Fu, 2008: Eddy-induced meridional heat transport in the ocean. *Geophys. Res. Lett.*, **35**, L20601, doi:10.1029/2008GL035490.

Watts, D., and W. E. Johns, 1982: Gulf Stream meanders: Observations on propagation and growth. *J. Geophys. Res.*, **87**, 9467–9476, doi:10.1029/JC087iC12p09467.

Zhai, X., and R. Greatbatch, 2006: Inferring the eddy-induced diffusivity for heat in the surface mixed layer using satellite data. *Geophys. Res. Lett.*, **33**, L24607, doi:10.1029/2006GL027875.